DESIGN OF MID-INFRARED MULTI-WAVELENGTH RADIATION THERMOMETER*

CONG Da-Cheng DAI Jing-Min SUN Xiao-Gang CHU Zai-Xiang
(School of Computer Science and Electronic Engineering, Harbin Institute of Technology, Harbin, Heilongjian 150001, China)

Abstract A brand-new kind of mid-infrared multi-wavelength radiation thermometer for the measurement of true temperature and emissivity near room temperature with high signal-to-noise ratio (SNR) was presented. By applying blazed grating and refractive-reflected optical system with high image quality and throughput, the temperature and emissivity were available simultaneously by the MCT semiconductor sensor array and electric system. Inner blackbody source was installed to compensate the surrounding temperature drift, and the temperature of field stop and aperture stop was controlled by a heat pipe to reduce the influence of stray radiation on temperature measurement. The main structures of optical and electric systems were described in detail.

Key words multi-wavelength radiation thermometry, low temperature measurement, emissivity, stray radiation.

中红外多波长辐射温度计的设计*

丛大成 戴景民 孙晓刚 褚载祥
(哈尔滨工业大学计算机与电气工程学院, 黑龙江, 哈尔滨, 150001)

摘要 介绍了以高信噪比同时测量近室温目标温度和光谱发射率的中红外多波长辐射温度计, 详细说明了其光学系统及电气系统设计. 采用高像质、大光通量的折反式光学系统和闪耀光栅分光系统, 通过多元碲镉汞探测器线列及电气系统, 可同时检测目标温度及发射率. 内置黑体炉和热管恒温视场光栏和孔径光栏减小了周围环境温度漂移及杂散光对温度测量的影响.

关键词 多波长辐射测温学, 低温温度测量, 发射率, 杂散光

Introduction

With the development of material science, it is important to measure the thermophysical properties such as temperature, emissivity and coefficient of thermal expansion for various materials at low temperature. And the measurements of true temperature and spectral emissivity near ambient conditions are especially crucial for the development of ablative and stealth materials which are often used in military and aerospace industries. However, some kinds of radiation thermometers available are only designed for the measurement of the properties near room temperature[1~5].

Multi-wavelength radiation thermometry has attracted people's attention mainly in the connection with the development of dynamic techniques for measurements of thermophysical properties of materials simultaneously[6~9]. During the past few decades, the measurements of thermophysical properties at low temperature were limited mainly by the techniques of optical design and detector manufacture. Hence, it is necessary to develop an instrument for that kind of measurement now.

In this paper the principles, optical design and electric system of a prototype mid-infrared multi-wavelength radiation thermometer, which has been developed for the measurements of true temperature and spectral emissivity near ambient conditions at the same time, are described in detail.

* The project supported by the National Natural Science Foundation of China (No. 69777020) and by the Special Foundation of Natural Excellent Dissertation for Degree of Docters (No. 199929)
Received 1999-11-30, revised 2000-05-17

* 国家自然科学基金(编号: 69777020)和高等学校全国优秀博士学位论文作者专项基金(编号: 199929)资助项目
稿件收到日期 1999-11-30, 修改稿收到日期 2000-05-17

1 Principles

In multi-wavelength radiation thermometry, the signal measured in channel i is given by

$$S_i = G_{\lambda_i} \int_{\Delta\lambda_i} \epsilon(\lambda_i, T)\tau(\lambda_i)\delta(\lambda_i)P(\lambda_i, T)d\lambda \quad (1)$$

where G_{λ_i} is the geometry factor involving the target area and the solid angle subtended by the entrance pupil of the instrument, $P(\lambda_i, T)$ is the Planck function of wavelength λ_i and temperature T, $\tau(\lambda_i)$ is the transmittance of optical system, $\delta(\lambda_i)$ is the spectral responsivity of the detector and $\Delta\lambda_i$ is the bandwidth.

The signal measured in channel i against a reference blackbody at a known temperature T_0 is given by

$$S_{i0} = G_{\lambda_i} \int_{\Delta\lambda_i} \tau(\lambda_i)\delta(\lambda_i)P(\lambda_i, T_0)d\lambda \quad (2)$$

Rearranging Eqs (1) and (2) with effective wavelength gives:

$$\frac{S_i}{S_{i0}} = \epsilon(\lambda_{ei}, T)\frac{P(\lambda_{ei}, T)}{P(\lambda_{ei}, T_0)} \quad (3)$$

Generally, the least square method has been used to process the data of the multi-wavelength thermometry, in which mathematical mode between spectral emissivity and wavelength must be assumed for a certain unknown material[10]. However, so far a universal assumption suitable for any material has not been found although the stepwise regression has been used[11].

At present, the artificial neural network has provided a range of new techniques for solving problems in pattern recognition and data processing[12, 13], so it is possible to solve the uncertain nonlinear relationship between the signal of each channel and the true temperature of the target. Backpropagation (BP) network based on gradient descent algorithm was experimentally verified in terms of data processing of multi-wavelength radiation thermometry for the first time by Sun[14] to develop an emissivity-independent radiation thermometer for the measurement of true temperature and spectral emissivity. After trained by a set of samples, the instrument will be ready to use. Another more powerful neural network, radial basis function (RBF) network[15], is proposed in this instrument to achieve better results.

2 Architecture of Optical Design

2.1 Optical design

Optical system design is the primary technique to develop the mid-infrared multi-wavelength radiation thermometer. The basic optical design of the new multi-wavelength radiation thermometer is shown in Fig. 1. The radiant flux emitted by the target is focused on the field stop 3 by the objective lens that is composed of crescent-shaped lens 1 with the diameter of 6.5cm and reflector 2. The former and the radiation emitted from the inner reference blackbody are focused on the chopper 14 by the condensing lenses 5 and 13, respectively, and reach the dispersing system by the collimating lens 7 alternatively. Finally, the blazed grating 8 splits the beam and dark chamber lens 10 projects the spectrum on the detector array 11.

2.2 Target

Since the spectral band of each channel is extracted from the total flux emitted by the target, it is allowed to disperse the flux exiting from the field stop and to locate it on the focal plane of the collimating lens. Then optimum throughput is achieved if the field stop has the same shape as the detector, consisting of a group of array elements. This shape is rectangular with the size of 0.8×1.0 mm^2 for each element.

2.3 Optical lens

The amount of radiant energy of targets near room temperature is comparatively weak and concentrated on mid-infrared range. Therefore, a refractive-reflected optical system is preferred for its outstanding characteristic of less attenuation in energy, large amount of luminous flux and high quality of image in mid-infrared multi-wavelength radiation thermometer[16]. The angle of aperture of image side, $\sin u'$, may be as large as 0.33.

The objective lens is composed of a ZnS lens with antireflection coating and a primary reflector plated with gold. Chromatic aberration and

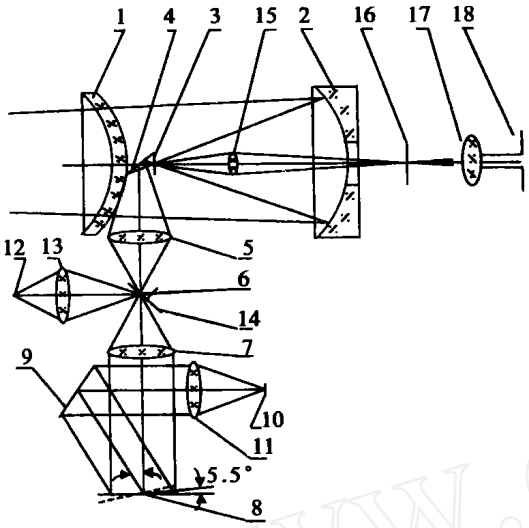

Fig. 1 Schematic diagram of optical system

1-crescent-shaped lens　2-primary reflector
3-field stop　4-secondary reflector
5-condensing lens　6-second image
7-collimating lens　8-blazed grating
9-reflector　10-dark chamber lens
11-third image and detector array
12-standard source　13-condensing lens
14-chopper　15-microscopical lens
16-image plane of microscope
17-eyepiece　18-exit pupil of eyepiece

图 1　光学系统原理图

1-新月型透镜　2-主反射镜　3-视场光阑
4-次反射镜　5-聚光镜　6-第二次像
7-准直物镜　8-闪耀光栅　9-反射镜
10-暗箱物镜　11-第三次像和探测器阵列
12-标准光源　13-聚光镜　14-调制盘
15-显微物镜　16-显微物镜像面
17-目镜　18-目镜出瞳

monochromatic aberration can be eliminated very well if the thickness of the ZnS lens is properly chosen. As visible light can pass through ZnS, aiming and focusing in visible light and infrared ranges simultaneously are realized by the aiming system. The focal distance of the objective lens is 80mm and the object distance is 500mm. Other optical lenses are made of germanium with antireflection coating and the total optical transmittance is 60%.

2.4　Reference source

Usually, for the measurement of near ambient conditions a reference blackbody with constant temperature is installed in the radiometers in order to compensate the drift of the surrounding temperature and temperature change of the chopper. In this instrument, heat pipe technique is introduced for making reference blackbody, which is compact and isothermal with this technique.

2.5　Blazed grating

The angle between facet and surface of the blazed grating is 9.5° and the inclination 5.5°, totally 15°. The angle between the direction of blaze and incidence is 30°. From above angles we get the formulation $d[\sin(30° - 5.5°) - \sin 5.5°] = K \times \lambda_b$, and the interval of the notch is $d \approx 0.031$, approximately 32 couples of line per millimeter. At this time the blazing wavelength $\lambda_b = 10\mu m$, i.e. we can achieve the spectrum scope of $10 \pm 5\mu m$.

2.6　Detector

HgCdTe is a kind of excellent semiconductor material for an infrared sensor. HgCdTe detectors can detect very small quantities of radiation at middle or long wavelength, thus measuring low temperature of an object. In order to realize high sensitivity, a metal dewar bottle detector array with D^* of $2.0 \times 10^{10} cmHz^{1/2}/W$ was used and the detector was cooled at the operating temperature of 77K by liquid nitrogen.

2.7　Stray radiation reduction

With low temperature multi-wavelength radiation thermometry, the temperature of the target is near the ambient condition, which makes that the stray radiation outside and intrinsic radiance of the instrument cannot be ignored. To reduce the effects of stray radiation in the temperature measurement, temperatures of several core optical components are controlled. In our new instrument, the temperature of field stop and aperture stop is con-

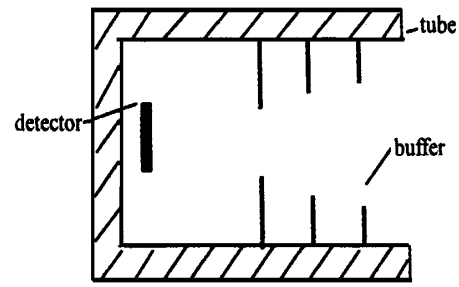

Fig. 2 Sketch map of a detector with cold buffer

图 2　带冷光阑的探测器示意图

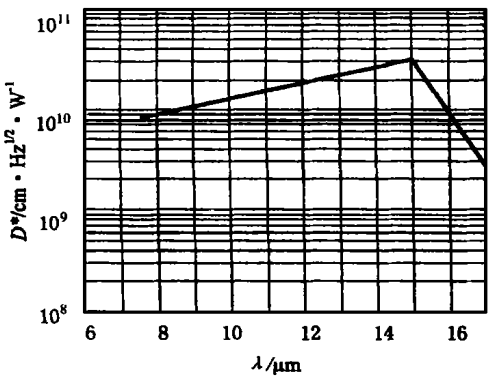

Fig. 3 D^* of HgCdTe detector

图3 碲镉汞探测器的探测率D^*

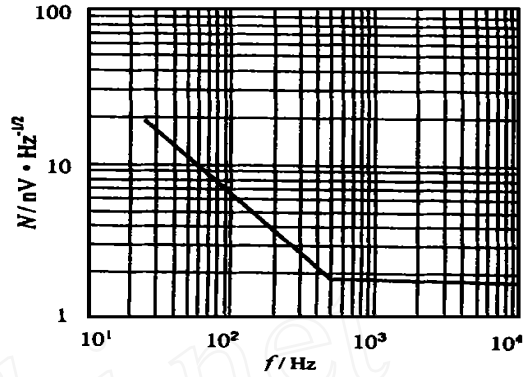

Fig. 4 Dependence of noise on frequency of HgCdTe detector

图4 HgCdTe探测器的噪声与频率关系

Table 1 Calculated results of SNR

表1 信噪比计算结果

Target temperature (℃)	λ_s= 5.5μm	λ_s= 7.0μm	λ_s= 9.5μm	λ_s= 11.5μm	λ_s= 13.0μm	λ_s= 14.5μm
15	4794.369	7272.453	6670.236	5119.487	3692.025	2620.837
16	4702.781	7112.433	6511.426	4991.542	3596.763	2551.714
17	4608.948	6949.819	6350.792	4862.505	3500.883	2482.235
18	4512.832	6784.582	6188.329	4732.375	3404.382	2412.402
19	4414.397	6616.705	6024.032	4601.165	3307.263	2342.221
20	4313.605	6446.172	5857.892	4468.864	3209.524	2271.685
21	4210.418	6272.960	5689.913	4335.478	3111.177	2200.800
22	4104.798	6097.049	5520.084	4201.008	3012.208	2129.565
23	3996.708	5918.418	5348.406	4065.452	2912.635	2057.985
24	3886.109	5737.051	5174.868	3928.812	2812.450	1986.058
25	3772.963	5552.928	4999.465	3971.095	2711.661	1913.791
26	3657.229	5366.023	4822.198	3652.287	2610.264	1841.182
27	3538.870	5176.322	4643.069	3512.407	2508.258	1768.234
28	3417.849	4983.816	4462.067	3371.445	2405.661	1694.945
29	3294.120	4788.467	4279.182	3229.405	2302.456	1621.319
30	3167.652	4590.268	4094.420	3086.286	2198.659	1547.362

trolled at 10℃ by heat pipe and the tube with cold buffers is installed in the front of the aperture of the detector as shown in Fig. 2. Therefore the sensitivity and stability of the instrument are improved.

2.8 Signal-to-noise ratio estimation

Prior to the practical design, the SNR of the instrument should be estimated to prove the feasibility. According to the specification of the detector, the detectivity of the HgCdTe sensor is typically 2.0×10^{10} as shown in Fig. 3 and the active area of the detector is $0.8\times0.8\text{mm}^2$. The $1/f$ noise is reduced to a minimum value at the chopping frequency of 800Hz as shown in Fig. 4. The SNR is calculated with the assumptions that the effective area of the target is $5.4\times6.7\text{mm}^2$, the central wavelengths are 5.5, 7.0, 9.5, 11.5, 13.0 and 14.5μm, respectively, with bandwidth $\Delta\lambda$= 1μm, spectral transmittance is 60% and the bandwidth of electric circuit is 100Hz. The calculation results of SNR of the six channels are shown in Table 1 with the temperatuer ranging from 15 to 30℃.

3 Electric design

Figure 5 shows a schematic diagram of an electronic system of the instrument. Alternated ra-

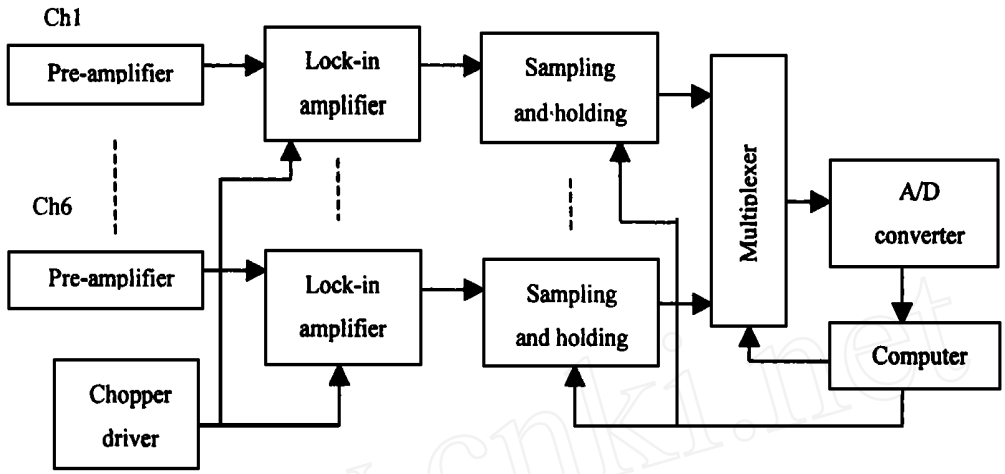

Fig. 5 Schematic diagram of electronic system
图 5　电路系统原理图

diation of 800Hz by the optical chopper is detected by the HgCdTe detector and amplified by the preamplifier with a bandpass filter. Lock-in amplifiers with the technique known as phase-sensitive detection (PSD) single out the component of the signal at the reference frequency and phase and convert the signal from AC to DC[17]. Thus, noises at frequencies other than the reference frequency are rejected and will not affect the measurement. Signals, which are proportional to the radiation intensity, can be read out in a sequence by a multiplexer. The sequential signal output is connected to an ADC.

4　Influence of temperature drift

In order to investigate the influence of temperature drift on measurements, experiments were carried out with three kinds of tubes, which were made of copper, aluminum and blackened copper, respectively. Keeping the blackbody temperature at 300K, the surrounding temperature inside the optical system changed from 313K to 353K measured by Pt100 thermal resistance embedded in the optical system. Figure 6 shows the comparison results. It is clear that the outputs using copper and aluminum tubes were higher than that of the blackened tube. Consequently, the blackened tube attenuates the influence of drift of surrounding temperature much more than the other two tubes.

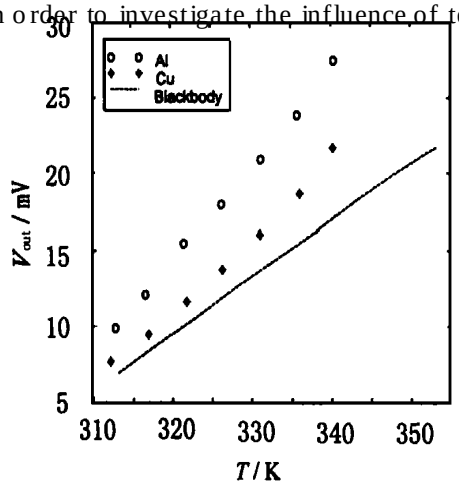

Fig. 6 Experiment result of temperature drift
图 6　温度漂移实验结果

5　Summary

A new kind of multi-wavelength radiation thermometer for the measurement of true temperature and near room temperature emissivity has been developed. The refractive-reflected optical system and the electronic system with lock-in amplifiers realized the characteristic of high throughput, less energy attenuation, high SNR, and aiming in visible light and infrared simultaneously. Great versatility can also be achieved by software operation. Experimental results showed that blackened tube with cold buffers was capable of compressing temperature drift compared with the other two kinds of material.

REFERENCES

[1] Iuchi T, Jono A. New radiation thermometer for near room temperature, *Measurement*, 1995, **16**: 257—263

[2] Inagaki T, Okamoto Y. Surface temperature measurement near ambient conditions using infrared radiometers with different detection wavelength bands by applying a gray-body approximation: estimation of radiation properties for non-metal surfaces, *NDT & E International*, 1996, **29**(6): 363—369

[3] Kurokawa K, Inagaki T, Masahiro A, *et al*. Temperature measurement at normal temperature condition by bicolored infrared radiometer in consideration of reflection from surroundings and its accuracy, *Trans Jpn. Soc Mech. Eng., Ser B*, 1996, **32**(4): 470—476

[4] LI Chun-Huai. Investigation of measurements of surface emissivity and temperature of terrestrial objects under usual conditions, *Chin. J. Infrared Res* (**李春槐 常温地物比辐射率和表面温度测量方法的研究**, **红外研究**), 1985, **4**: 361—369

[5] ZHANG Cai-Gen. The measurement of the surface temperature via the brightness method, *Acta Physica Sinica* (**张才根 常温物体表面真实温度的亮度法测量**, **物理学报**), 1982, **31**(9): 1191—1197

[6] Gathers G R. Analysis of multi-wavelength pyrometry using nonlinear least square fits and Monte-Carlo methods, *Int. J. Thermal Physics*, 1992, **13**(3): 539—554

[7] Levendis Y A, Estrada K R, Hott H C. Development of multicolor pyrometers to monitor the transient response of burning carbonaceous particles, *Rev. Sci. Instrum.*, 1992, **63**(7): 3608—3622

[8] Cezairliyan A, Foley G M, Morse M S, *et al*. Six-wavelength millisecond resolution pyrometer, *Temp., its Measur. and Contr. in Sci. and Ind.*, 1993, **6**: 757—762

[9] Ruffino G, Chu Z X, Kang S G, *et al*. Multi-wavelength pyrometer with photodiode array, *Temp., its Measur. and Contr. in Sci. and Ind.*, 1993, **6**(2): 807—810

[10] Coates P B. The least-square approach to multi-wavelength pyrometry, *High Temp. High Press*, 1988, **20**: 433—441

[11] SUN Xiao-Gang, DAI Jing-Min, CONG Da-Cheng. Theoretical study of multi-wavelength radiation thermometry—autosearch for emissivity expression general, *J. Infrared Millim. Waves* (**孙晓刚, 戴景民, 丛大成, 多光谱辐射测温的理论研究——发射率模型的自动判别, 红外与毫米波学报**), 1998, **17**(3): 18—23

[12] Carroll S M, Dicknson W. Construction of neural nets using random transform, *IJCNN*, 1989, **1**: 607—611

[13] Hornik K. Approximation capabilities of multilayer feedback network, *Neural Networks*, 1991, **4**(2): 251—257

[14] SUN Xiao-Gang. Study of the theory and experiment of the multispectral thermometry, Ph. D. Thesis, Harbin Institute of Technology (**孙晓刚 多光谱测温的理论及实验研究**, **哈尔滨工业大学博士学位论文**), 1998

[15] Chris M Bishop. Neural networks and their applications, *Rev. Sci. Instrum.*, 1994, **65**(6): 1803—1830

[16] LI Zheng-Zhi. *Infrared Optical System*. Changsha: Publishing House of University of National Defence (**李正直 红外光学系统 长沙: 国防大学出版社**), 1986, 296

[17] ZENG Qing-Yong. *Faint Signal Processing*. Hangzhou: Publishing House of Zhejiang University (**曾庆勇. 微弱信号处理 杭州: 浙江大学出版社**), 1986